Canadian Science Publishing
NRC Research Press journals | Publishing Services

Canadian Journal of Physics
Revue canadienne de physique

Energy, fine structure, hyperfine structure, and transitions for the high-lying multi-excited 4Pe,o states of B-like ions

Journal:	*Canadian Journal of Physics*
Manuscript ID	cjp-2015-0609.R3
Manuscript Type:	Article
Date Submitted by the Author:	10-Feb-2016
Complete List of Authors:	Zhang, Chun Mei; Beijing Institute of Technology, physics Sun, Yan; Xuzhou Institute of Technology Chen, Chao; Beijing Institute of Technology, physics Wang, Feng; Beijing Institute of Technology, Laser Micro/Nano Fabrication Laboratory, School of Mechanical Engineering Shao, Bin; Beijing Institute of Technology, physics Gou, Bing Cong; Beijing Institute of Technology, physics
Keyword:	B-like ions, transition wavelength, fine structure, QED corrections, hyperfine structure

Energy, fine structure, hyperfine structure, and transitions for the high-lying multi-excited $^4P^{e,o}$ states of B-like ions

Chun Mei Zhang[a], Yan Sun[b], Chao Chen[a], Feng Wang[c], Bin Shao[a], and Bing Cong Gou[a,*]

a School of Physics, Beijing Institute of Technology, Beijing 100081, P.R. China

b School of Mathematical and Physical Science, Xuzhou Institute of Technology, Xuzhou 221111, P.R. China

c Laser Micro/Nano Fabrication Laboratory, School of Mechanical Engineering, Beijing Institute of Technology, Beijing 100081, P.R. China

Abstract

The energies of the high-lying multi-excited states $1s^22s2pnl$ and $1s^22p^2nl$ $^4P^{e,o}$ ($n \geq 2$) for B-like C^+, N^{2+}, F^{4+} and Mg^{7+} ions are calculated using Rayleigh–Ritz variation method with multiconfiguration interaction, and the inclusion of mass polarization and relativistic corrections. The fine structure and hyperfine structure for these systems are investigated using first-order perturbation theory. The configuration structure of the high-lying multi-excited series is identified not only by energy but also by its contribution to normalization of the angular-spin components, and it is further tested by the addition of relativistic corrections and fine structure splittings. Transition wavelengths including the quantum electrodynamic effects and higher-order relativistic corrections are determined.

Keywords: B-like ions; transition wavelength; fine structure; QED corrections.
PACS: 31.15.ac; 32.70.Cs; 31.15.aj; 31.30.jc

1. Introduction

The high-lying multi-excited states of B-like ions have high orbital, spin, and angular momentum quantum numbers and are therefore complex five-electron atomic systems. Studying these systems will help us to understand better atomic structure, since five-electron system have complicated electronic correlation effects. Investigations on the spectra of B-like ions are of considerable interest for the study and modeling of high-temperature astrophysical and laboratory plasmas. Extensive experiments [1-7] and theoretical investigations [8-24] have been done on the

* Email:goubing@sina.com

multi-excited states of B-like ions. Experimentally, early in 1956, Burke [1] identified the energy levels of the $1s^2 2s2p3s\ ^4P^o$ state for neutral B. In the 1970s, investigations in the wavelength range 450 - 5200 Å using beam-foil technique [2] and flash pyrolysis technique [3] served to identify many new spectrum lines for neutral B. After that, Buchet [4] studied the spectrum of N^{2+} and identified some newly observed lines with beam-foil technique. Later, the emission spectrum of doubly ionized nitrogen, N^{2+}, has been studied by Michels [5] at high resolution in the extreme ultraviolet, from 150 to 500 Å and 87 new lines reported. Recently, D´ esesquelles [6] identified some far UV spectra of F^{4+} ions using collision spectroscopy.

Theoretically, in 1995, Merkelis [8] studied the energy spectra and transitions in the B isoelectronic sequence (Z = 8-26) between the levels with configurations $2s^2 2p$, $2s2p^2$ and $2p^3$ using the stationary second-order many-body perturbation theory (MBPT). In 1998, Safronova [9] obtained energies and fine structure splittings for the $2s^2 3l$, $2s2p3l$, $2p^2 3l$ configurations of B-like ions (Z = 6-30) using relativistic many-body perturbation theory (RMBPT). Recently, In 2004, Froeser Fischer et al [10] calculated the energy levels, transition rates of levels up to $2s^2 3d$ in the spectra of B-like ions (Z = 5-14) using the multiconfiguration Hartree-Fock (MCHF) method, and G. Correge [11] presented oscillator strengths and transition rates between levels belonging to the set of $2s^2 2p$, $2s2p^2$, $2p^3$, $2s^2 3l$ (l = 0, 1, 2) configurations for each of the C^+, N^{2+} using the computer code CIV3. In 2010, Per Jönsson [12] calculated the energy levels, hyperfine interaction constants, Landé g_J factors, and transition probabilities of the levels $2p^3$, $2s^2 3l$, $2s2pnl$ using the multiconfiguration Dirac–Hartree–Fock(MCDHF). Using relativistic configuration interaction (RCI), energy calculations on $2s^2 2p$, $2s2p^2$, $2p^3$ configurations of B-like ions were performed by P. Rynkun [13] in 2012. S. Verdebout [14] reported hyperfine interaction constants and Landé g_J-factors of the $1s^2 2s2p^2\ ^4P^e$ states of B-like ions by RCI method in 2014. However, so far, only few hyperfine structure constants for the multi-excited $^4P^{e,o}$ states of B-like ions have been reported and they require further investigation. Other methods have also been employed to study the energy and transitions of these quartet states of the B, i.e. configuration interaction (CI) [15, 16], multi-channel R-Matrix method [17], superstructure code [18], and 1/Z perturbation theory method [19]. Most of the investigations on B-like ions are focused on low-lying excited states, a few on high-lying excited states.

In this work, the energy levels and transitions for the high-lying excited quartet states $1s^2 2s2pnl$

and $1s^22p^2nl$ ($5 \geq n \geq 2$) $^4P^{e,o}$ of the B-like ions are studied by the Rayleigh-Ritz variational method with multiconfiguration interaction wave functions. The first-order perturbation theory is used to compute the relativistic effects and the mass polarization. The structure of the Configurations of the high-lying multi-excited series of the B-like ions are further examined with relativistic perturbation corrections and fine structure splittings. The hyperfine parameters for these systems are also calculated. The transitions from $1s^22s2pnl$ and $1s^22p^2nl$ ($5 \geq n \geq 2$) $^4P^{o,e}$ to $1s^22s2p^2$ $^4P^e$ and $1s^22s2p3s$ $^4P^o$ are calculated respectively. Transition wavelength is also calculated including Quantum electrodynamic effects (QED) and high-order relativistic corrections by the screened hydrogenic method.

2. Theory

In order to calculate the non-relativistic energy of the B-like ions, the basic wave function Ψ_b can be written as

$$\Psi_b(1,2,3,4,5) = A\sum_i C_i \Phi_{n(i),l(i)}(1,2,3,4,5), \tag{1}$$

$$\Phi_{n(i),l(i)}(1,2,3,4,5) = \phi_{n(i),l(i)}(R) Y^{LM}_{l(i)}(\Omega)\chi_{SS_z}, \tag{2}$$

where A is the antisymmetrization operator, Y^{LM} are the spherical harmonics and radial basis functions $\phi_{n(i),l(i)}(R)$ are the Hartree products of Slater orbitals,

$$\phi_{n(i),l(i)}(R) = \prod_{j=1}^{5} r_j^{n_j} \exp(-\alpha_j r_j). \tag{3}$$

The angular and spin wave function can be simply represented by

$$\begin{aligned} l_i &= \{[(l_1,l_2)l_{12},l_3]l_{123},l_4\}l_{234},l_5, \\ \chi_{ss_z} &= \{[(s_1,s_2)s_{12},s_3]s_{123},s_4\}s_{1234},s_5. \end{aligned} \tag{4}$$

One set of nonlinear parameters α_j is used for each angular-spin component. The linear parameters C_i and the nonlinear parameters α_j are determined variationally. Using the Rayleigh-Ritz variational method, we determine the basic wave function Ψ_b and the corresponding upper bounds of the energy E_b.

In order to saturate the functional space, the restricted variational method [25] is used to

improve energy E_b. The basic wave function Ψ_b is used as a single and leading term in an improved wave function Φ, which is given by

$$\Phi(1,2,3,4,5) = D_0\Psi_b(1,2,3,4,5) + \Psi_2(1,2,3,4,5), \quad (5)$$

where

$$\Psi_2(1,2,3,4,5) = A\sum_{i=1}^{I} D_i\Phi_{n(i),l(i)}(1,2,3,4,5). \quad (6)$$

Here, Ψ_2 has essentially the same form than Ψ_b, but the nonlinear parameters are completely different from those of Ψ_b. $D_i's$ are the linear parameters, D_0 is normalized parameter

Each of the nonlinear parameters in the basic functions of Ψ_2 is optimized in the restricted variational calculation. The total nonrelativistic energy is obtained by adding the improvement from restricted variation ΔE_{RV}. Then the nonrelativistic energy is added as $E_b + \Delta E_{RV}$.

The total energy is further improved by including the mass polarization effect and the relativistic corrections. The relativistic perturbation operators considered in this work are the corrections to the kinetic energy, the Darwin term, and the electron-electron contact term and orbit-orbit interaction. Explicit expressions of these operators are given in Ref. [26], and they will not be repeated here.

The fine structure perturbation operators [25] are given by

$$H_{FS} = H_{SO} + H_{SOO} + H_{SS}, \quad (7)$$

where the spin–orbit, spin–other-orbit and spin–spin operators are

$$H_{so} = \frac{Z}{2c^2}\sum_{i=1}^{5}\frac{\mathbf{l}_i\cdot\mathbf{s}_i}{\mathbf{r}_i^3}, \quad (8)$$

$$H_{soo} = -\frac{1}{2c^2}\sum_{\substack{i,j=1\\ i\neq j}}^{5}[\frac{1}{r_{ij}^3}(\mathbf{r}_i-\mathbf{r}_j)\times\mathbf{p}_i]\cdot(\mathbf{s}_i+2\mathbf{s}_j), \quad (9)$$

$$H_{ss} = \frac{1}{c^2}\sum_{\substack{i,j=1\\ i<j}}^{5}\frac{1}{r_{ij}^3}[\mathbf{s}_i\cdot\mathbf{s}_j - \frac{3(\mathbf{r}_{ij}\cdot\mathbf{s}_i)(\mathbf{r}_{ij}\cdot\mathbf{s}_j)}{r_{ij}^2}], \quad (10)$$

$\mathbf{s}_i$ and $\mathbf{l}_i$ are the spin and the orbital angular momentum of the *i*th electron. To calculate the fine structure splitting, the *LSJ* coupling scheme is used. The fine structure levels are calculated by

first-order perturbation theory.

The hyperfine structure of atomic energy levels is caused by the interaction between the electrons and the electromagnetic multipole moments of the nucleus. The leading terms of this interaction are the magnetic dipole and the electric-quadrupole moments. For an *N*-electron system, the hyperfine interaction Hamiltonian can be represented as follows [27]:

$$H_{hfs} = \sum_{k=1} \mathbf{T}^{(k)} \cdot \mathbf{M}^{(k)}, \tag{11}$$

Where $\mathbf{T}^{(k)}$ and $\mathbf{M}^{(k)}$ are the spherical tensor operators of rank k in the electronic and nuclear spaces, respectively. The $k = 1$ term shows the magnetic-dipole interaction between the magnetic field generated by the electrons and nuclear magnetic-dipole moments, the $k = 2$ term representing the electric quadrupole interaction between the electric-field gradient from the electrons and the nonspherical charge distribution of the nucleus. The contributions from higher-order terms are much smaller and can be neglected. Hyperfine interaction couples electronic angular momentum **J** and nuclear angular momentum **I** to a total angular momentum **F=I+J**. The uncoupling and coupling hyperfine constants are defined in atomic units as [28]

$$a_c = \left\langle \gamma LSM_L M_S \left| \sum_{i=1}^{5} 8\pi\delta^3(r_i)\mathbf{s}_0(i) \right| \gamma LSM_L M_S \right\rangle \text{ (Fermi contact)} \tag{12}$$

$$a_{sd} = \left\langle \gamma LSM_L M_S \left| \sum_{i=1}^{5} 2\mathbf{C}_0^{(2)}(i)\mathbf{s}_0(i) r_i^{-3} \right| \gamma LSM_L M_S \right\rangle \text{ (spin-dipolar)}, \tag{13}$$

$$a_l = \left\langle \gamma LSM_L M_S \left| \sum_{i=1}^{5} \mathbf{l}_0^{(1)}(i) r_i^{-3} \right| \gamma LSM_L M_S \right\rangle \text{ (orbital)}, \tag{14}$$

$$b_q = \left\langle \gamma LSM_L M_S \left| \sum_{i=1}^{5} 2\mathbf{C}_0^{(2)}(i) r_i^{-3} \right| \gamma LSM_L M_S \right\rangle \text{ (electric-quadrupole)}, \tag{15}$$

and

$$A_J = \frac{\mu_I}{I} \frac{1}{\left[J(J+1)(2J+1)\right]^{1/2}} \left\langle \gamma J \left\| \mathbf{T}^{(1)} \right\| \gamma J \right\rangle, \tag{16}$$

$$A_{J,J-1} = \frac{\mu_I}{I} \frac{1}{\left[J(2J-1)(2J+1)\right]^{1/2}} \left\langle \gamma J \left\| \mathbf{T}^{(1)} \right\| \gamma (J-1) \right\rangle, \tag{17}$$

$$B_J = 2Q \left[\frac{2J(2J-1)}{(2J+1)(2J+2)(2J+3)} \right]^{1/2} \left\langle \gamma J \left\| \mathbf{T}^{(2)} \right\| \gamma J \right\rangle. \tag{18}$$

Where μ_I is the nuclear magnetic moment. Q is the nuclear electric-quadrupole moment.

To estimate QED effects and higher-order relativistic contributions for these multiexcited quartet states of B-like ions, the screened hydrogenic formulae have been used. The theories of screened hydrogenic have been discussed in detail elsewhere [29]. Finally, the QED effects and higher-order relativistic corrections are obtained by

$$\Delta E_{QED} = \sum_{i=1}^{5} \Delta E_{QED}(n_i l_i j_i, LSJ), \tag{19}$$

$$\Delta E_{HO} = \sum_{i=1}^{5} \Delta E_{HO}(n_i l_i j_i, LSJ). \tag{20}$$

3. Results and discussion

The high-lying excited quartet states of B-like ions are complex five-electron atomic systems and the correlation effects between the electrons are extremely complicated. There are several possibilities to couple each orbital angular and spin angular in total angular momentum. In order to get a high-quality wave function, the number of angular-spin components ranges in this work from 53 to 99, and the number of linear parameters ranges from 1545 to 3260. In the $^4P^o$ states, which parity is odd, the important angular series [l_1, l_2, l_3, l_4, l_5] are [000l, l+1], [001l, l], [011l, l+1], [012l, l], [001l, l+2], [111l, l], and so on. In the $^4P^e$ states, which parity is even, the important angular series [l_1, l_2, l_3, l_4, l_5] are [000l, l], [011l, l], [002l, l], [001l, l+1], [111l, l+1], and so on. In this last case, the value of l goes from 1 to 6, since the energy contribution of the set with $l > 6$ is very small and it can be neglected. In order to saturate the wave functional space and improve the energy E_b obtained from Ψ_b, the restricted variational method is used to calculated energy contributions from each chosen angular-spin series. The total nonrelativistic energy is then obtained by adding the improvement from restricted variation ΔE_{RV}. Then, the nonrelativistic energy is given by $E_b + \Delta E_{RV}$. Table 1 gives energies for the ground state $1s^2 2s^2 2p\ ^2P$ of B-like C^+, N^{2+}, F^{4+}, and Mg^{7+} ions. The nonrelativistic energies, mass polarization, and relativistic correction contributions for the high-lying multi-excited states $1s^2 2s 2pnl$ and $1s^2 2p^2 nl\ ^4P^{e,o}(m)$ ($n \geq 2$) (m = 1-5) of B-like C^+, N^{2+}, F^{4+}, and Mg^{7+} ions are presented in Table 2. The energy improvement ΔE_{RV} ranges from -69 μ a. u. to -395 μ a. u. according to the restricted variational method. The high-lying ^4P states of B are not calculated because these states are not stable.

In Table 2, the high-lying excited states of these B-like ions are numbered according to their positions in the series. The lowest is assigned as (1). As it is shown in Table 2, our calculated relativistic energies of the high-lying excited $^4P^{e,\ o}$ states are in good agreement with the experimental results compiled by NIST [30] and slightly lower than those theoretical data from RMBPT [9], MCHF [10], and RCI [13]. For example, the energy of the $1s^22s2p4d\ ^4P^o$ state for F^{4+} in this work is 3.836659 a.u., which is in good agreement with NIST data 3.836660 a.u., which is micro hartree accurate. Note that for the high-m states, such as $1s^22s2p5p\ ^4P^e(5)$ for N^{2+}, $2s2p4p\ ^4P^e(4)$ for F^{4+}, and $2s2p4p\ ^4P^e(5)$ for Mg^{7+}, no experimental and theoretical data are available to compare with at present.

Each high-lying excited $^4P^{e,o}$ state of the B-like ions is first identified by energy and by the percentage contribution to the normalization of the various angular-spin components and second, tested by relativistic perturbation corrections and fine structure splitting. For instance, from the point of view its relative contribution to the normalization of the angular-spin components, *ssssp* is the main configuration of the $^4P^o(m)$ (m = 1 ,3, 5) states, while *ssspd* is the main configuration of the $^4P^o(m)$ (m = 2, 4) states in N^{2+}. Therefore, the lowest energy state of the *ssssp* configuration series is assigned to the $1s^22s2p3s\ ^4P^o(1)$, and the lowest state of the *ssspd* configuration series is assigned to the $1s^22s2p3d\ ^4P^o(2)$, respectively. We note that the relativistic correction of the $1s^22s2snl$ state is larger than the one of the $1s^22s2pnl$ state, which in turn is larger than the one of the $1s^22p^2nl$ state. As it is shown in Table 2, *ssspp* is the main configuration of both $1s^22s2p3p\ ^4P^e$ and $1s^22p^23s\ ^4P^e$ states in F^{4+} ion. The relativistic correction of $1s^22s2p3p\ ^4P^e$ state has the value −0.079679 a.u. is apparently larger than the value -0.075423a.u. of $1s^22p^23s\ ^4P^e$ state. Therefore, identifying $1s^22s2p3p$ as $^4P^e(2)$ and $1s^22p^23s$ as $^4P^e(3)$ for F^{4+} ion is reasonable. The other ions are also identified by using a similar procedure.

FIGURE 1. Fine structure splitting $v_{1.5\text{-}0.5}$ and $v_{2.5\text{-}1.5}$ (cm^{-1}) for the multi-excited states $^4P^o(m)$ (m=1-5) of B-like ions.

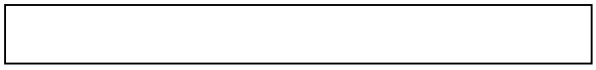

FIGURE 2. Fine structure splitting $v_{1.5\text{-}0.5}$ and $v_{2.5\text{-}1.5}$ (cm^{-1}) for the multi-excited states $^4P^e(m)$ (m=1-5) of B-like ions.

The fine structure splitting of the multiexcited quartet states for B–like C^+, N^{2+}, F^{4+}, and Mg^{7+} ions are presented in Table 3. The relativistic energies of Table 2 are the centre-of-gravity energies. The fine structure splittings are resulted from the effects of the spin-orbit, spin-other-orbit and spin-spin interaction. As Table 3 shows, the fine structure splittings in this work are in good agreement with other theoretical [9, 10, 13, 21] and experimental [5, 30] data. We also note that the fine structure calculation results give $| v_{2.5-1.5} | > | v_{1.5-0.5} |$ for the high-lying excited $^4P^{e,o}$ series of these systems. Figures 1 and Figure 2 give the systematical changes of the fine structure splittings of the high-lying excited states $^4P^o(m)$ and $^4P^e(m)$ ($m = 1-5$) along with the m increasing for the C^+, N^{2+}, F^{4+}, and Mg^{7+} ions, respectively. Both figures show that fine structure splittings $v_{2.5-1.5}$ and $v_{1.5-0.5}$ of the B isoelectronic sequence have a similar behavior when m increase. As it is shown in Figure 1, the drastic changes of the fine-structure splittings at the $^4P^o(2)$ and $^4P^o(4)$ of this $^4P^o$ series are reasonable considering the assignment of configuration structures for these system in Table 2. Here, the main configuration (*ssspd*) of the $^4P^o(2)$ and the $^4P^o(4)$ states is completely different from the main configuration (*ssssp*) of the $^4P^o(1)$, $^4P^o(3)$ and $^4P^o(5)$ states in the C^+ and N^{2+} ions. For F^{4+} and Mg^{7+} ions, the drastic changes of the fine-structure splittings of the $^4P^o$ series at the $^4P^o(2)$ and $^4P^o(5)$ are also reasonable considering the assignment of configuration structures for these systems. In Table 1, the main configuration (*ssspd*) of the $^4P^o(2)$ and $^4P^o(5)$ for F^{4+} and Mg^{7+} is completely different from the main configuration (*ssssp*) of the $^4P^o(1)$, $^4P^o(3)$ and (*ssppp*) of the $^4P^o(4)$ for F^{4+}, and the main configuration (*ssssp*) of the $^4P^o(1)$, $^4P^o(4)$ and (*ssppp*) of the $^4P^o(3)$ for Mg^{7+}, respectively. In Figure 2 one can see that, the drastic changes of the fine-structure splittings of the even parity ^4P series for these systems are also reasonable according to the assignment of configuration structures in Table 2. As described in Eqs. (8–10), we note that the fine structure splitting depend on the orbital and spin angular moments, and the investigation of the fine structure splitting could be very useful to further checks of the configuration structures.

FIGURE 3. Hyperfine parameters (a.u.) and hyperfine coupling constants (GHz) for the multi-excited states $1s^2 2s 2p 3s\ ^4P^o$ for B-like ions.

In Table 4, the hyperfine structures of the high-lying excited states $^4P^{e,o}(m)$ (m = 1−3) for B-like C^+, N^{2+}, F^{4+}, and Mg^{7+} ions are shown. In this table, the hyperfine structure parameters: Fermi contact a_c, spin dipolar a_{sd}, orbital a_l, electric-quadrupole b_q and hyperfine coupling constants: A_J and B_J are given. The nuclear spin I, the nuclear magnetic dipole moment μ_I, and the electric-quadrupole moment Q of the B-like ions taken from Ref. [28] are listed in table 6. In Table 4, we note that the absolute value of the hyperfine structure parameters of the high-lying excited $^4P^{e,o}$ states for these B-like ions with increasing nuclear charge numbers Z are becoming larger, showing the coupling between nuclear spin and the electronic angular momentum becomes more apparent. Let's Take $1s^22s2p3s\ ^4P^o$ state for example, as shown in Figure 3, the Fermi contact a_c is much larger and change faster than orbital parameter a_l, and the absolute value of electric-quadrupole b_q change much faster than spin dipolar a_{sd}. As it is shown in Table 4, our calculated results of the hyperfine coupling constants for $1s^22s2p^2\ ^4P^e$ and $1s^22s2p3s\ ^4P^o$ states are in good agreement with the Verdebout's data [14] employing the RCI method and Per Jönsson's data [12] using the MCDHF method. To our knowledge, no other calculations of hyperfine structures of these high-lying excited systems have been yet reported, therefore we were not able to compare with other results.

Table 5 gives the radiative transition rates A_{ik} and transition wavelengths for the transition between multi-excited quartet states $^4P^{o,e}(m)$ (m = 1-5) and the lowest states $1s^22s2p^2\ ^4P^e$ and $1s^22s2p3s\ ^4P^o$ of the $^4P^{e,o}$ series for B-like C^+, N^{2+}, F^{4+}, and Mg^{7+} ions, respectively. In this work, the radiative transition rates from dipole length A_l, dipole velocity A_v, and dipole acceleration A_a formulae are in a reasonable agreement with each other. The good agreement between the length, velocity, and acceleration results can be used as the indicator of the accuracy of wave function. Also the calculated transition rates are in good agreement with the experimental and other theoretical results. As shown in Table 5, the transition wavelengths λ including the QED effect agree well with the experimental results [4, 5, 6, 7, 30]. For example, in this work, the calculated transition wavelength between the $2p^23d\ ^4P^e$ state and the $2s2p3s\ ^4P^o$ state of Mg^{7+} ions has the value 27.562 nm, which is in good agreement with 27.562 nm by the NIST [30] data collection,

and the transition wavelength between the $2s2p3s\ ^4P^o$ state and the$2s2p^2\ ^4P^e$ state for N^{2+} ion is 43.430 nm, which is in good agreement with 43.4 nm reported by Buchet [4] using beam-foil technique. The wavelength discrepancy between our results and those of NIST data [30] is of about 0.01% to 1.4%. Table 5 shows that the QED corrections of these multi-excited quartet states are more important than the higher order relativistic corrections and innegligible. For instance, the transition wavelength $2p^23d\ ^4P^e \rightarrow 2s2p3s\ ^4P^o$ in the F^{4+} ion is calculated combining the wavelength 41.859 nm and $\Delta\lambda_{QED}$ 0.0067 nm is 41.866 nm which agrees well with experimental data [30] 41.878 nm and if we add the corrections including $\Delta\lambda_{QED}$ and $\Delta\lambda_{HQ}$ 0.0001 nm then the value is also 41.866 nm. The transition rates and wavelengths of some high-lying excited quartet states in the systems have not been reported before, and need to be further investigated.

4. Conclusion

In this work, the energy levels, fine structure, hyperfine structure, transitions of the high-lying excited quartet states for the B isoelectronic sequence have been studied. Some energy levels and most of the hyperfine structure constants for the high-lying excited quartet states of the B-like ions are reported for first time. The present studies indicate that relativistic corrections and fine structure splittings play an important role in testing the structure of the configurations of the systems. Calculated transition wavelengths agree well with the experimental values when the QED effect and higher order relativistic corrections are included. This study of the high-lying multi-excited quartet states for B-like ions should be useful for identifying these highly ionized spectra in the future.

Acknowledgements

This work is supported by the National Natural Science Foundation of China under Grants No. 11474020 and 11375025 and by the Special Foundation for theoretical physics Research Program of China under Grant No. 11547145.

References

[1] E.W. Burke; Jr., J.E. Mack, J. Opt. Soc. Am. **1956**, 46, 100-105.

[2] I. Martinson; W.S. Bickel, J. Opt. Soc. Am. **1970**, 60, 1213-1220.

[3] R.A. Roig; G. Tondello, J. Phys. B: Atom. Molec. Phys. **1976**, 9, 2373-2378.

[4] J. P. Buchet; M. C. Poulizac, M. Carre, J. Opt. Soc. Am. **1972**, 62, 623-626.

[5] D. J. Michels, J. Opt. Soc. Am. **1974**, 64, 1164-1174.

[6] J. D´ esesquelles; M.C. Buchet-Poulizac; J. Bernard; R. Br´edy; L. Chen; A. Denis; S. Martin; H.G. Berry, Phys. Scr. **2001**, T92, 290-293.

[7] Jan Bromander, Phys. Scr. **1971**, 4, 61-63.

[8] G. Merkelis; M.J. Vilkas; G. Gaigalas; R. Kisielius, Phys. Scr. **1995**, 51, 233-251.

[9] U.I. Safronova; W.R. Johnson , M.S. Safronova, At. Data Nucl. Data Tables **1998**, 69, 183-215.

[10] C. Froese Fischer; G. Tachiev, At. Data Nucl. Data Tables **2004**, 87, 1-184.

[11] G. Corrégé; A. Hibbert, At. Data Nucl. Data Tables **2004**, 86, 19-34.

[12] P. Jönsson; J. Li, G. Gaigalas; C.Z. Dong, At. Data Nucl. Data Tables **2010**, 96, 271-298.

[13] P. Rynkun; P. Jönsson; G. Gaigalas; C. F. Fischer, At. Data Nucl. Data Tables **2012**, 98, 481-556.

[14] S. Verdebout; C. Naz´e; P. J¨onsson; P. Rynkun; M.Godefroid; G. Gaigalas, At. Data Nucl. Data Tables **2014**, 100, 1111-1155.

[15] A.W. Weiss, Phys. Rev. **1969**, 188, 119-130.

[16] G. Correg´e; A. Hibbert´, J. Phys. B: At. Mol. Opt. Phys. **2002**, 35, 1211-1227.

[17] N. J. Wilson; K. L. Bell; C. E. Hudson, A&A. **2005**, 432, 731-736.

[18] M.E. Galav´ıs; C. Mendoza; C.J. Zeippen, A&A Suppl. Ser. **1998**, 131, 499-522.

[19] U. I. Safronova, A. S. Shlyaptseva, Physica Scripta. , **1996**, 54, 254-270

[20] G. Tachiev; C. Froese Fischer, J. Phys. B: Atom. Molec. Phys. **2000**, 33, 2419-2435.

[21] U.I. Safronova, T. Kato, Phys. Scr. **1996**, 53, 461-472.

[22] G. A. Odintzova; A. R. Striganov, J. Phys. Chem. Ref. Data **1979**, 8, 63-67.

[23] Y. Sun; F. Chen; L. Zhuo; B. C. Gou, Int. J. Quantum Chem. **2012**, 112, 1114-1121.

[24] Chun Mei Z ha ng, Chao Chen, Yan Sun, Bing Cong Gou, Bin Shao, Eur. Phy s. J. D. **2015**, 69, 105-112

[25] K. T. Chung; X. W. Zhu, Phys Rev A. **1993**, 48, 1944-1954.

[26] B.F. Davis; K.T. Chung, Phys. Rev. A. **1984**, 29, 1878-1882.

[27] H.Y. Yang; K.T. Chung, Phys. Rev. A. **1995**, 51, 3621-3629.

[28] P. Raghavan, At. Data Nucl. Data Tables **1989**, 42, 189-291.

[29] K.T. Chung; X.W. Zhu; Z.W. Wang, Phys. Rev. A. **1993**, 47, 1740-1751.

[30] http://www.nist.gov/pml/data/asd.cfm, Sept. 16, 2014.

Table 1

Energies (a.u.) for the ground state $1s^2 2s^2 2p\ ^2P$ of B-like C^+, N^{2+}, F^{4+}, and Mg^{7+} ions.

Z	$\Delta E_b + \Delta E_{RV}$	$\Delta E_{mp} + \Delta E_{rel}$	E_{total}		
			This work	NIST	Ref. [19]
6	-37.42935	-0.01480	-37.44415	-37.443389	
7	-52.96358	-0.02809	-52.99167		
9	-92.29324	-0.08387	-92.37711		-92.376445[a]
12	-171.92203	-0.30138	-172.22341	-172.198353	-172.198625[a]

Table 2

Energies (a.u.) of the multi-excited $1s^2 2s2pnl$ and $1s^2 2p^2 nl\ ^4P^{e,o}(m)$ (m = 1-5) states of B-like C^+, N^{2+}, F^{4+}, and Mg^{7+} ions.

States	$\Delta E_b + \Delta E_{RV}$	*spp/ppd/sdd* or *ssp/spd/ppp*	$\Delta E_{mp} + \Delta E_{rel}$	E_{total}	Energy relative to ground state		
					This work	NIST[a]	others
			C^+				
$2s2p^2\ ^4P^e(1)$	-37.23387	995/003/002	-0.01358	-37.24745	0.19670	0.19610	0.19646[b]
							0.19635[f]
							0.19480[g]
							0.19550[i]
							0.19502[j]
$2s2p3p\ ^4P^e(2)$	-36.57985	994/004/000	-0.01371	-36.59355	0.85059	0.84958	0.84859[b]
							0.86521[g]
							0.86521[e]
$2s2p4p^4P^e(3)$	-36.44331	995/003/000	-0.01368	-36.45699	0.98716	0.98598	0.98638[b]
$2s2p5p^4P^e(4)$	-36.38458	996/003/000	-0.01361	-36.39828	1.04586	1.04326	
$2s2p6p^4P^e(5)$	-36.35350	996/003/000	-0.01366	-36.36716	1.07699	1.07286	
$2s2p3s^4P^o(1)$	-36.66850	983/009/008	-0.01381	-36.68231	0.76184	0.76099	0.77453[e]
							0.76138[f]
							0.76160[b]
							0.76072[j]
$2s2p3d^4P^o(2)$	-36.52263	010/982/003	-0.01367	-36.53629	0.90785	0.90610	0.93205[e]
							0.90173[b]
$2s2p4s\ ^4P^o(3)$	-36.47364	981/016/003	-0.01380	-36.48748	0.95666	0.95503	0.95292[b]
$2s2p4d^4P^o(4)$	-36.42254	028/968/000	-0.01371	-36.43625	1.00790	1.00620	1.00321[b]
$2s2p5s^4P^o(5)$	-36.39888	969/028/002	-0.01385	-36.41273	1.03142	1.02883	
			N^{2+}				
$2s2p^2\ ^4P^e(1)$	-52.70451	996/002/001	-0.02675	-52.73120	0.26042	0.26099	0.26125[f]
							0.26099[c]
							0.25889[g]
							0.26058[h]
							0.26075[i]
							0.26039[j]
$2s2p3p\ ^4P^e(2)$	-51.51873	995/004/000	-0.02699	-51.54572	1.44596	1.44605	1.44606[c]
							1.45925[e]
$2s2p4p^4P^e(3)$	-51.23583	996/003/000	-0.02692	-51.26275	1.72893	1.72858	1.72859[c]
$2p^2 3s\ ^4P^e(4)$	-51.14070	996/007/001	-0.02564	-51.16633	1.82534	1.82567	1.83358[e]
$2s2p5p^4P^e(5)$	-51.11189	996/003/000	-0.02682	-51.13871	1.85390		
$2s2p3s^4P^o(1)$	-51.65434	983/008/009	-0.02709	-51.68143	1.31024	1.31063	1.31064[c]
							1.32170[e]

							1.31128[f]
							1.31040[j]
$2s2p3d\,^4P^o(2)$	-51.43281	010/983/005	-0.02678	-51.45963	1.53205	1.53208	1.53209[c]
							1.55274[e]
$2s2p4s\,^4P^o(3)$	-51.28493	986/009/004	-0.02716	-51.31209	1.67958	1.67965	1.67968[c]
$2s2p4d\,^4P^o(4)$	-51.20351	011/985/000	-0.02666	-51.23082	1.76085	1.76005	1.76005[c]
$2s2p5s\,^4P^o(5)$	-51.13605	980/015/005	-0.02700	-51.16302	1.82866	1.82708	1.82708[c]
			F^{4+}				
$2s2p\,^{24}P^e(1)$	-91.90638	998/001/000	-0.07936	-91.98574	0.39136	0.39269	0.38882[d]
							0.39312[f]
							0.39229[h]
$2s2p3p\,^4P^e$ (2)	-89.24116	996/003/000	-0.79679	-89.32084	3.05627		3.06916[e]
$2p^23s\,^4P^e(3)$	-88.72910	992/006/001	-0.07542	-88.80453	3.57258	3.57465	3.58126[e]
$2s2p4p\,^4P^e(4)$	-88.51769	988/011/000	-0.07923	-88.59692	3.78019		
$2p^23d\,^4P^e(5)$	-88.38275	032/966/000	-0.07422	-88.45698	3.92013	3.91992	3.92814[e]
$2s2p3s\,^4P^o(1)$	-89.46598	983/007/009	-0.08028	-89.54626	2.83084	2.83113	2.83960[e]
							2.83226[f]
$2s2p3d\,^4P^o(2)$	-89.09817	009/983/006	-0.07928	-89.17744	3.19966	3.20224	3.21678[e]
$2s2p4s\,^4P^o(3)$	-88.60732	919/008/073	-0.07929	-88.68660	3.69050	3.69000	
$2p^23p\,^4P^o(4)$	-88.54866	199/008/79	-0.07562	-88.62428	3.75283	3.75111	3.74651[e]
$2s2p4d\,^4P^o(5)$	-88.46117	006/989/004	-0.07928	-88.54045	3.83666	3.83666	
			Mg^{7+}				
$2s2p^2\,^4P^e(1)$	-171.35020	999/000/000	-0.27404	-171.62423	0.59918	0.59999	0.59841[d]
							0.60161[f]
							0.60005[h]
$2s2p3p\,^4P^e(2)$	-165.41879	996/003/000	-0.27110	-165.68990	6.53352		6.54128[e]
$2p^23s\,^4P^e(3)$	-164.70788	993/006/000	-0.25727	-164.96515	7.25827	7.24471	7.26348[e]
$2p^23d\,^4P^e(4)$	-164.14976	006/993/000	-0.25173	-164.40149	7.82193	7.82057	7.82904[e]
$2s2p4p\,^4P^e(5)$	-163.65947	996/003/000	-0.26885	-163.92833	8.29509		
$2s2p3s\,^4P^o(1)$	-165.78178	983/009/000	-0.27547	-166.05927	6.16618	6.16625	6.17338[e]
							6.16989[f]
$2s2p3d\,^4P^o(2)$	-165.19163	008/985/006	-0.26955	-165.46118	6.76224	6.76238	6.77290[e]
$2p^23p\,^4P^o(3)$	-164.43762	011/008/980	-0.25428	-164.69190	7.53152	7.52907	7.53181[e]
$2s2p4s\,^4P^o(4)$	-163.79869	989/005/006	-0.27110	-164.06980	8.15362	8.15070	
$2s2p4d\,^4P^o(5)$	-163.57564	007/991/000	-0.26930	-163.84493	8.37848	8.37936	

[a]Ref.[28].[b]Ref.[20]. [c]Ref.[5].[d]Ref.[8] [e]Ref.[9] [f]Ref.[10][g]Ref.[11].[h]Ref.[13]. [i]Ref.[16]. [j]Ref.[12].

Table 3

Fine structure splittings $\nu_{J-J'}$(cm^{-1}) of the high-lying excited states $^4P^{e,o}(m)$ (m = 1−5) for B-like C^+, N^{2+}, F^{4+}, and Mg^{7+} ions.

States	$\nu_{1.5-0.5}$		$\nu_{2.5-1.5}$	
	this work	others	this work	others
		C^+		
$2s2p\,^{24}P^e(1)$	22.04	22[e], 21[d], 22.22[c], 22.02[g]	28.10	28.30[e], 35[d], 28.45[c], 28.19[g]
$2s2p3p\,^4P^e(2)$	15.81	16.34[e], 25[d], 16[b]	22.52	22.33[e], 25[d], 25[b]
$2s2p4p\,^4P^e(3)$	15.07	16.75[e], 67[d]	22.06	20.98[e], 17[d]
$2s2p5p\,^4P^e(4)$	13.61		22.69	20.1[e]
$2s2p6p\,^4P^e(5)$	13.50		22.51	
$2s2p3s\,^4P^o(1)$	26.01	24 [b],23.7[c],27[d], 23.6[e], 23.63[g]	43.35	45[b],45.2[c], 44[d], 44.98[e], 44.99[g]

$2s2p3d\ ^4P^o(2)$	- 13.40	-12[b], -12[d],-13.76[e]	- 22.33	- 22[b],-22.0[d], -21.25[e]
$2s2p4s^4P^o(3)$	26.26	27[d], 24.1[e]	43.77	45[d], 45.86[e]
$2s2p4d\ ^4P^o(4)$	- 12.46	-12[d],-12.92[e]	- 20.77	- 13[d],-20.46[e]
$2s2p5s^4P^o(5)$	21.14	23.16[e]	40.40	43.82[e]
		N^{2+}		
$2s2p^{24}P^e(1)$	59.25	59.9[a], 59.7[e],59.85[c] 59.7[f],59.4[g]	80.47	81.2[a], 81.1[e], 81.07[c], 81.9[f],80.61[g]
$2s2p3p\ ^4P^e(2)$	41.02	43.5[a], 42.6[e], 43[b]	60.36	58.9[a], 59[e], 62[b]
$2s2p4p^4P^e(3)$	36.01	44.8[a]	60.02	52.9[a]
$2p^23s^4P^e(4)$	61.43	66.7[a], 68[b]	102.38	99.3[a], 103[b]
$2s2p5p^4P^e(5)$	35.51		59.19	
$2s2p3s^4P^o(1)$	67.13	62.5[a],63[b],62.55[c], 62.1[e],62.45[g]	111.89	115.8[a],116[b],115.94[c], 115.4[e],115.67[g]
$2s2p3d\ ^4P^o(2)$	- 33.92	-35.1[a], -32[b], -35[e]	- 56.54	-54.6[a],-56 [b], -54.7[e]
$2s2p4s^4P^o(3)$	68.47	62.7[a], 63.9[e]	114.12	116.5[a], 118[e]
$2s2p4d\ ^4P^o(4)$	- 3.03	-32.5[a], -32.5[e]	- 55.05	- 54.1[a], -54.1[e]
$2s2p5s^4P^o(5)$	68.02	71.7[a], 71.7[e]	113.37	119.3[a], 118.9[e]
		F^{4+}		
$2s2p^{24}P^e(1)$	225.36	254.96[c],253.9[f]	375.59	363.71[c],364.0[f]
$2s2p3p\ ^4P^e(2)$	157.69	184[b]	262.81	249[b]
$2p^23s^4P^e(3)$	269.66	263.80[e], 274[b]	413.79	406.0[e], 418[b]
$2s2p4p^4P^e(4)$	145.51		242.52	
$2p^23d^4P^e(5)$	- 15.23	-112 [b]	- 192.05	- 198[b]
$2s2p3s^4P^o(1)$	271.38	258[b],257.6[c], 256.5[e]	452.30	468[b], 467.98[c], 468[e]
$2s2p3d\ ^4P^o(2)$	- 133.02	-130[b], -154[e]	- 221.71	- 209[b], - 202[e]
$2s2p4s^4P^o(3)$	268.60	363.5[e]	447.67	392[e]
$2p^23p^4P^o(4)$	174.30	135[b], 39[e]	290.55	149[b], 250[e]
$2s2p4d\ ^4P^o(5)$	135.92	100[e]	226.53	328[e]
		Mg^{7+}		
$2s2p^2\ ^4P^e(1)$	1032.2	1157.10[c], 1145[f]	1720.34	1672.36[c], 1669[f]
$2s2p3p\ ^4P^e(2)$	699.96	886[b]	1166.62	1022[b]
$2p^23s^4P^e(3)$	1108.6	1193[b]	1847.78	1802[b]
$2p^23d^4P^e(4)$	- 508.98	- 444 [b]	- 848.30	- 825 [b]
$2s2p4p^4P^e(5)$	632.37		1053.95	
$2s2p3s^4P^o(1)$	1168.3	1107[b],1109[c],1140[e]	1947.26	2024[b],2031.2[c],2020[e]
$2s2p3d\ ^4P^o(2)$	- 547.10	-478[b], -490[e]	- 911.84	- 744[b],- 730[e]
$2p^23p^4P^o(3)$	686.38	499[b]	1143.96	1021[b]
$2s2p4s^4P^o(4)$	1182.8		1971.14	
$2s2p4d\ ^4P^o(5)$	- 572.29		- 953.82	

[a]Ref.[5].[b]Ref.[9].[c]Ref.[10].[d]Ref.[20].[e]Ref.[28].[f]Ref.[13].[g]Ref.[12].

Table 4

Hyperfine parameters (a.u.) and hyperfine coupling constants (GHz) for the multi-excited states $^4P^{e,o}(m)$(m=1-3) forB-like C^+, N^{2+}, F^{4+}, and Mg^{7+} ions.The numbers in brackets Indicate the powers of 10.

States	a_c	a_l	a_{sd}	b_q	A_J			B_J	
					J=2.5	J=1.5	J=0.5	J=2.5	J=1.5
					C^+				
$2s2p^{24}P^e$	47.085	2.232	0.468	0.867	0.987	1.015	2.210		
					0.933[b]	0.948[b]	2.059[b]		
$2s2p3p^4P^e$	51.012	1.525	0.316	0.603	1.011	1.106	2.446		
$2s2p4p^4P^e$	52.328	1.449	0.298	0.592	1.030	1.136	2.516		
$2s2p3s\ ^4P^o$	58.544	2.705	- 0.565	- 1.051	1.162	1.492	2.584		
					1.166[b]	1.495[b]	2.592[b]		
$2s2p3d\ ^4P^o$	52.025	- 1.309	- 0.065	- 0.123	0.857	1.104	2.693		

$2s2p4s\ ^4P^o$	54.377	2.723	- 0.574	- 1.055	1.088	1.403	2.374		
					N^{2+}				
$2s2p^{24}P^e$	84.790	4.619	0.958	1.813	0.522	0.525	1.134	- 8.22[-3]	6.58[-3]
					0.507[b]	0.506[b]	1.090[b]	- 8.5[-3][b]	6.8[-3][b]
$2s2p3p^4P^e$	90.158	3.095	0.642	1.234	0.521	0.561	1.236	- 5.60[-3]	4.48[-3]
$2s2p4p^4P^e$	94.130	2.894	0.591	1.173	0.538	0.587	1.296	- 5.32[-3]	4.25[-3]
$2s2p3s\ ^4P^o$	108.720	5.334	- 1.104	- 2.077	0.624	0.802	1.367	9.42[-3]	- 7.54[-3]
					0.625[b]	0.804[b]	1.368[b]	9.8[-3][b]	- 7.9[-3][b]
$2s2p3d\ ^4P^o$	91.800	- 2.488	- 0.134	- 0.255	0.432	0.559	1.369	- 1.15[-3]	- 9.25[-4]
$2s2p4s\ ^4P^o$	98.386	5.416	- 1.131	- 2.124	0.572	0.740	1.218	9.63[-3]	- 7.71[-3]
					F^{4+}				
$2s2p^{24}P^e$	207.265	13.360	2.746	5.266	17.112	16.666	35.618		
					17.366[a]	16.956[a]	36.299[a]		
$2s2p3p^4P^e$	223.731	8.833	1.822	3.452	17.120	18.110	39.679		
$2p^23s^4P^e$	26.047	14.639	3.013	5.790	5.287	1.803	1.631		
$2s2p3s^4P^o$	274.576	14.676	- 3.027	- 5.795	20.723	26.733	44.477		
$2s2p3d\ ^4P^o$	228.508	- 6.588	- 0.376	- 0.728	13.904	18.106	44.498		
$2s2p4s\ ^4P^o$	220.479	14.471	2.902	- 5.687	17.085	22.183	34.552		
					Mg^{7+}				
$2s2p^{24}P^e$	580.270	40.149	8.200	15.876	-3.160	-3.035	- 6.449	- 0.750	0.600
					-3.200[a]	-3.082[a]	- 6.570[a]	- 0.758[a]	0.604[a]
$2s2p3p^4P^e$	605.842	26.324	5.411	10.404	-3.055	-3.189	- 6.958	- 0.491	0.393
$2p^23s^4P^e$	102.950	42.533	8.720	16.934	-1.118	-0.488	- 0.637	- 0.799	0.640
$2s2p3s\ ^4P^o$	760.070	42.529	- 8.677	- 16.817	-3.754	-4.847	- 7.960	0.794	- 0.635
$2s2p3d\ ^4P^o$	610.690	- 18.520	- 1.117	- 2.178	-2.405	-3.147	- 7.755	0.103	- 0.082
$2p^23p\ ^4P^o$	- 38.061	26.188	- 3.349	- 6.471	-0.132	-0.191	1.152	0.306	- 0.244

[a]Ref [14], [b]Ref [12]

Table 5

Radiative transition rates A_{ik} (s^{-1}),and wavelengths λ(nm) for the multi-excited quartet states of B-like C^+, N^{2+}, F^{4+}, and Mg^{7+} ions. The numbers in brackets indicate the powers of 10.

transitions	$A_l/A_v/A_a$	λ			
		This work	NIST[b]	QED	HQ
		C^+			
$2s2p^{24}P^e\rightarrow$					
$2s2p3s\ ^4P^o$	1.34[9]/1.31[9]/3.45[8]	80.720	80.662	0.0002	0
	8.48[8][b]	80.642[e]			
	2.52[9][e]				
	6.24[8][g]				
$2s2p3d\ ^4P^o$	2.10[9]/2.09[9]/2.21[9]	64.140	64.164	0	0
	2.20[9][b]	64.620[f]			
	1.031[10][f]				
$2s2p4s\ ^4P^o$	3.03[8]/3.00[8]/2.69[8]	60.019	60.038	0.0002	0
	3.63[8][b]				
$2s2p4d\ ^4P^o$	9.66[8]/9.53[8]/9.60[8]	56.227	56.247	0.0001	0
	1.05[9][b]				
$2s2p5s\ ^4P^o$	3.41[8]/3.30[8]/2.40[8]	54.760	54.718	0.0002	0
	1.44[8][b]				
$2s2p3s\ ^4P^o\leftarrow$					
$2s2p3p\ ^4P^e$	9.00[7]/9.04[7]/4.24[8]	513.7342	514.685	- 0.0038	- 0.0002
		514.18[h]			
$2s2p4p^4P^e$	2.22[6]/2.25[6]/4.49[6]	202.364	202.659	- 0.0003	0.0002
$2s2p5p^4P^e$	3.49[6]/4.08[6]/5.77[5]	160.537	161.532	- 0.0002	0
$2s2p6p^4P^e$	3.32[6]/3.41[6]/1.37[7]	144.683	146.204	- 0.0002	0.0004

		N^{2+}			
$2s2p^{24}P^{e}\rightarrow$					
$2s2p3s\ ^{4}P^{o}$	4.26[9]/4.29[9]/2.90[9]	43.430	43.410	- 0.0001	0
	4.798[9][b]	43.394[e]			
	1.302[10][e]	43.410[d]			
	1.968[9][g]	43.40[c]			
$2s2p3d\ ^{4}P^{o}$	1.01[10]/1.00[10]/1.03[1	35.863	35.847	0	0
	1.10 [10][b]	35.847[d]			
$2s2p4s\ ^{4}P^{o}$	1.20[9]/1.23[9]/1.06[9]	32.126	32.119	0	0
	1.44[9][b]	32.134[d]			
$2s2p4d\ ^{4}P^{o}$	3.90[9]/3.89[9]/3.93[9]	30.390	30.396	0	0
	4.70[9][b]	30.395[d]			
$2s2p5s\ ^{4}P^{o}$	3.62[8]/3.72[8]/2.94[8]	29.070	29.095	0.0001	0
	6.904[8][b]	29.095[d]			
$2s2p3s\ ^{4}P^{o}\leftarrow$					
$2s2p3p\ ^{4}P^{e}$	1.78[8]/1.79[8]/3.00[7]	335.981	336.708	0.0110	0.0050
$2s2p4p^{4}P^{e}$	8.90[7]/8.36[7]/6.69[7]	108.905	109.097	0.0014	0.0007
$2p^{2}3s\ ^{4}P^{e}$	2.10[9]/1.99[9]/2.31[9]	88.521	88.531	0.0059	- 0.0005
$2s2p5p^{4}P^{e}$	1.58[7]/1.22[7]/6.48[6]	84.016		0	-0.0004
		F^{4+}			
$2s2p^{24}P^{e}\rightarrow$					
$2s2p3s\ ^{4}P^{o}$	2.02[10]2.01[10]/2.13[10	18.684	18.699	- 0.0001	0.0001
	6.08[10][e]	18.680[a]			
		18.681[e]			
$2s2p3d\ ^{4}P^{o}$	6.38[10]/6.37[10]/6.47[1	16.237	16.229	0	0
		16.220[a]			
$2s2p4s\ ^{4}P^{o}$	1.20[9]/1.23[9]/1.06[9]	13.820	13.828	0	0.0001
$2p^{2}3p^{4}P^{o}$	4.75[9]/5.18[9]/4.68[9]	13.579	13.577	0.0005	0
$2s2p4d^{4}P^{o}$	2.15[10]/2.09[10]/2.21[1	13.235	13.252	0	0
$2s2p3s\ ^{4}P^{o}\leftarrow$					
$2s2p3p\ ^{4}P^{e}$	3.55[8]/3.70[8]/1.16[9]	202.271		0.0224	0.0009
$2p^{2}3s^{4}P^{e}$	2.94[9]/2.90[9]/5.08[9]	61.472	61.325	0.0119	- 0.0004
$2s2p4p^{4}P^{e}$	1.08[9]/9.93[8]/2.48[8]	48.029		0.0013	0.0001
$2p^{2}3d^{4}P^{e}$	1.46[8]/9.20[7] /2.62[8]	41.859	41.878	0.0067	0.0001
		Mg^{7+}			
$2s2p^{24}P^{e}\rightarrow$					
$2s2p3s\ ^{4}P^{o}$	9.07[10]/9.09[10]/8.64[1	8.189	8.191	- 0.0002	0
	9.25[10][c]9.24[10][b]	8.183[e]			
$2s2p3d\ ^{4}P^{o}$	3.54[11]/3.54[11]/3.56[11	7.404	7.399	0	0
	3.53[11][b]				
$2p^{2}3p\ ^{4}P^{o}$	7.70[10]/7.80[10]/7.69[1	6.596	6.580	0.0005	0
$2s2p4s\ ^{4}P^{o}$	2.12[10]/2.15[10]/2.11[10	6.037		0	0
$2s2p4d\ ^{4}P^{o}$	1.19[11]/1.20[11]/1.19[11	5.864	5.861	0	0
$2s2p3s\ ^{4}P^{o}\leftarrow$					
$2s2p3p\ ^{4}P^{e}$	6.51[8]/6.60[8]/1.10[8]	123.441		0.0419	- 0.0010
$2p^{2}3s^{4}P^{e}$	4.38[9]/4.36[9]/8.22[9]	41.674	42.279	0.0221	- 0.0003
	4.43[9][b]				
$2p^{2}3d^{4}P^{e}$	3.26[7]/3.06[7]/4.01[7]	27.562	27.562	-0.0496	-0.0576
	6.52[7][b]				
$2s2p4p^{4}P^{e}$	9.57[9]/9.58[9]/7.06[9]	21.397		0.0013	0

[a]Ref.[6]. [b]Ref.[28]. [c]Ref.[4]. [d]Ref.[5]. [h]Ref.[7]. [e]Ref.[10]. [f]Ref.[20].[g]Ref.[12].

Table 6

nuclear spin I, the nuclear magnetic dipole moment μ_I（nm）,andthe electric-quadrupole moment$Q$(b) for B isoelectronic sequence

ion	I	μ_I	Q
$^{13}C^{+}$	0.5	0.702411	0
$^{14}N^{2+}$	1	0.403761	0.0193

$^{19}F^{4+}$	0.5	2.628868	0
$^{25}Mg^{7+}$	2.5	- 0.855450	0.2010

Figure 1

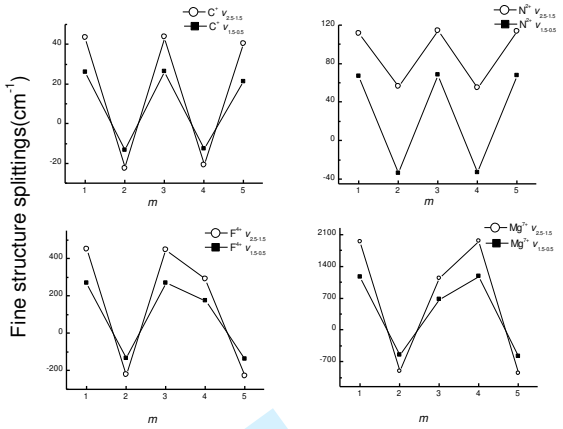

Figure 2

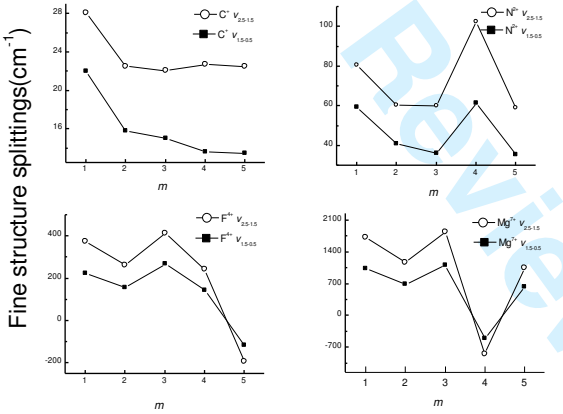

Figure 3